# Time–Delayed Feedback Control: Theory and Application

Wolfram Just[*], Ekkehard Reibold[†], and Hartmut Benner[‡]
*Institut für Festkörperphysik, Technische Universität Darmstadt*
*Hochschulstraße 6, D–64289 Darmstadt, Germany*

**Abstract**

Control of chaos is one of the most prominent applications of nonlinear dynamics. A conceptually very fruitful strategy proposes time–delayed differences of measured signals as control forces. Such approaches are simple to implement even in ultrafast experimental systems and can be applied if no mathematical modelling is available. As a drawback the control performance is difficult to understand theoretically since the whole dynamics is governed by a time delay system. Recently, some progress has been achieved and features of the control scheme have been understood on a general level, e.g. which type of periodic orbits is accessible to delayed feedback control, which feature of the measured power spectrum signals whether the control works successfully, and how control loop latency, which plays an important role in ultrafast experimental systems, affects the limits of control. We illustrate these points on several experimental systems, e.g. electronic circuits operating at MHz time scales. In addition, we dwell on high power ferromagnetic resonance in YIG spheres where the complex internal system dynamics does not allow for a simple modelling in terms of equations of motion. The dynamics of the magnetisation in strong microwave pumping fields is utilised for control purposes.

## 1 Introduction

Since world war II the topic of control has developed to one of the most prominent fields in engineering and applied mathematical sciences. Nowadays a vast amount of literature is available including modern approaches to control theory. At the beginning of the nineties physicists began to invade this field starting from the observation

[*]e–mail: wolfram@chaos.gwdg.de, present address: MPISF, Bunsenstraße 10, D–37073 Göttingen, Germany
[†]e–mail: Ekkehard.Reibold@physik.tu-darmstadt.de
[‡]e–mail: benner@hrzpub.tu-darmstadt.de

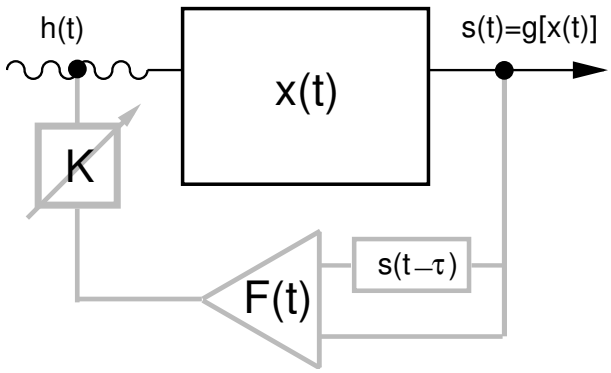


Figure 1: Setup for time–delayed feedback control experiment. $h(t)$ denotes some external parameter or driving field and $s(t)$ a scalar output signal. The control loop is displayed in gray.

that in nonlinear chaotic systems the huge number of different unstable orbits can be stabilised by applying tiny control forces. Although the scheme proposed in [1] is quite standard from the point of view of control theory, the new aspect i.e. the stabilisation of different dynamical states with almost vanishing forces has stimulated an ongoing avalanche of publications and it is hopeless to give even a crude overview over this literature. Roughly speaking the approaches can be grouped in two classes. The schemes based on [1] and its variants require specific knowledge about the internal dynamics. Usually one obtains such information by mathematical modelling or some kind of phase space reconstruction techniques (cf. [2]). However, in fast systems or systems which are sensitive to environmental changes one deserves for strategies which do not rely on fancy data processing tools but can be applied on–line. In such a context the time–delayed feedback method as proposed in [3] is quite useful for stabilising periodic states. Such schemes are robust and have been applied in a variety of experimental systems [4]. Unfortunately a more detailed understanding of the control mechanism is difficult since differential difference equations are involved, and only recently some progress has been achieved.

## 2 Theoretical analysis

Within a formal setting control means that one applies an external force $F(t)$ to a dynamical system in order to drive the internal degrees of freedom, $\boldsymbol{x}(t)$, towards a preferred state. In terms of equations of motion such a setting means

$$\dot{\boldsymbol{x}}(t) = \boldsymbol{f}\left(\boldsymbol{x}(t), KF(t)\right) \quad , \tag{1}$$

where for convenience an amplification factor $K$ for the control force is introduced. Control schemes differ by the recipes to generate the control force and the coupling of

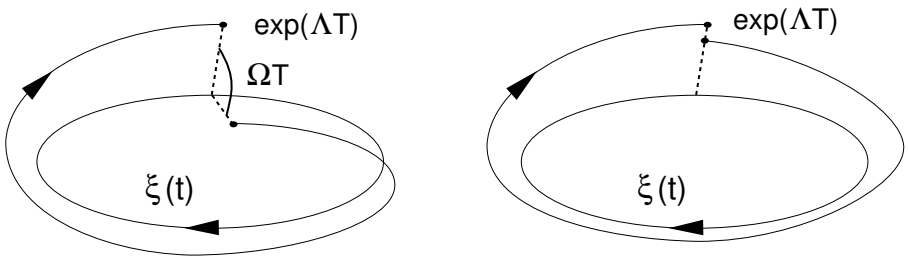


Figure 2: Trajectory in the vicinity of a periodic orbit for $\Omega \neq 0$ (left) and $\Omega = 0$ (right).

the force to the internal degrees of freedom. Unfortunately, the equations of motion are often unknown in applications, and an appropriate control scheme has to be worked out. If one focuses on the stabilisation of periodic orbits, i.e. unstable solutions $\boldsymbol{\xi}(t) = \boldsymbol{\xi}(t+T)$ of eq.(1) for $K = 0$, a particularly simple rule was proposed in [3]. It uses the plain time series of a scalar output signal $s(t) = g[\boldsymbol{x}(t)]$, and an appropriate force is generated by a time–delayed difference

$$F(t) = g[\boldsymbol{x}(t)] - g[\boldsymbol{x}(t-\tau)] \quad . \tag{2}$$

The whole setup which follows from the above considerations is sketched in Fig. 1. If we take as granted that the delay $\tau$ is adjusted to an integer multiple of the period, e.g. $\tau = T$, then the force (2) vanishes in the case of successful control, i.e. if the periodic orbit is finally reached.

In order to analyse the control performance the stability of the orbit subjected to control has to be discussed. This is usually done within the framework of linear stability analysis. If we consider trajectories in the vicinity of the periodic orbit $\boldsymbol{\xi}$, then in linear order the time evolution can be decomposed into eigenmodes

$$\boldsymbol{x}(t) - \boldsymbol{\xi}(t) \simeq \exp[(\Lambda + i\Omega)t]\boldsymbol{Q}(t), \quad \boldsymbol{Q}(t) = \boldsymbol{Q}(t+T) \quad . \tag{3}$$

Here the periodicity of the eigenmode $\boldsymbol{Q}(t)$ accounts for the periodic motion of the orbit, and the real and imaginary part of the so–called Floquet exponent $\Lambda + i\Omega$ determines expansion from and the revolution around the periodic orbit, respectively (cf. Fig. 2). Control becomes successful if the real part $\Lambda$ changes sign from positive to negative values. Inserting the ansatz (3) into the full equation of motion (1), (2) one ends up with a rather complicated eigenvalue problem. An explicit solution requires detailed knowledge of the equations of motion, but the structure of the force (2) already poses a constraint on the control performance [5]. Control can only be achieved if at the onset ($\Lambda = 0$) a finite torsion ($\Omega \neq 0$) is present. Such a feature can even be understood in a geometric way. Consider a trajectory in the vicinity of the periodic orbit. Points on such a trajectory become infinitesimally close after one period if control would set in without torsion, i.e. $\Lambda = 0$ and $\Omega = 0$ (cf. Fig. 2). But then the control force (2) which is just proportional to the distance of these points

vanishes before the desired orbit is reached and no stabilisation can be achieved. In addition with more sophisticated arguments such a feature yields constraints on the Floquet exponents of the uncontrolled system [6].

Beyond such topological arguments one can even derive within some approximation a closed form for the eigenvalue equation. The approximation is valid either if the control amplitude is not too large or in the limit of a mean field coupling. Specialising to the case that the free orbit flips its neighbourhood during one turn, i.e. the Floquet exponent has imaginary part $\omega = \pi/T$, the characteristic equation reads [5]

$$\Lambda\tau + i\Omega\tau = \lambda\tau + i\pi - (-\tau\chi')\,K\left[1 - e^{-\Lambda\tau - i\Omega\tau}\right], \quad (\tau = T) \quad . \tag{4}$$

Here $\lambda$ denotes the Lyapunov exponent of the free orbit and the only system dependent parameter $\chi'$ includes all the details of the internal dynamics and the coupling of the control force. Stability properties, in particular the dependence of the Floquet exponents on the control amplitude $K$, is now fairly easy to analyse and extensive comparison with experimental data will be done in the following section.

Finally we remark that the theoretical approach just sketched is not limited to the simple control scheme given by eq.(2). In fact the analysis of e.g. extended control schemes, control domains, or the influence of control loop latency goes along the same lines and for the interested reader we will quote the appropriate references within the proper context.

## 3 Experiments

We report on three different experimental examples where the predicted features of time–delayed feedback control could be observed in detail: (i) a nonautonomous electronic circuit, (ii) an autonomous electronic circuit, (iii) spin–wave instabilities in high power ferromagnetic resonance on YIG spheres. All three systems show chaotic oscillation on a $\mu s$ time scale. Therefore, analog delay lines were utilised for constructing the control device which allows a control force of the form $F(t) = -K[U(t) - (1-R)S(t-\tau)]$, $S(t) = U(t) + RS(t-\tau)$ with delay time $\tau = 10\text{ns} \ldots 21\mu\text{s}$ and a *memory parameter* $R = 0 \ldots 1$. This corresponds to the so–called *extended time delay autosynchronisation* method [7]. For $R = 0$ one obtains the simple feedback scheme of eq.(2).

### *3.1 Nonlinear diode resonator*

A simple nonautonomous system is the nonlinear diode resonator illustrated in Fig. 3. The circuit, consisting of a capacity diode (1N4005), an inductor ($47\mu$H) and a resistor ($36\Omega$), was sinusoidally driven at fixed frequency (800kHz). Without control the system undergoes a period doubling cascade to chaos on variation of the driving amplitude $U_A$. This guarantees a nonzero torsion ($\omega = \pi/T$) of the unstable periodic orbits. Therefore, the orbits should be accessible to time–delayed feedback control.

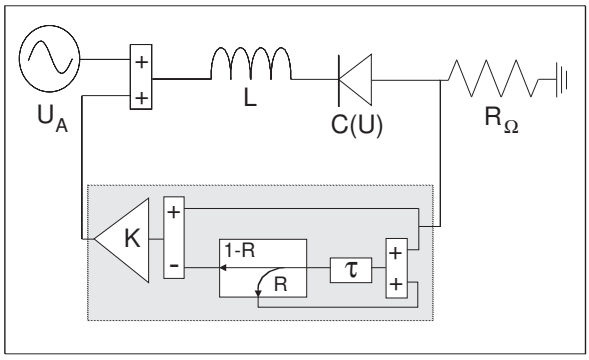


Figure 3: Experimental setup of the nonlinear diode resonator with extended time delay feedback device.

Stabilisation of the unstable period–1 orbit by means of eq.(2) is possible for control amplitudes $K > K^{(fl)} \approx 34$. The decay rate $\Lambda$ and frequency $\Omega$ in dependence of control amplitude $K$ were obtained from the transient dynamics of the control signal (cf. Fig. 4). For comparison with our theoretical prediction (4) we determined the two parameters $\chi'\tau$ and $\lambda\tau$ from the experimental values of $K^{(fl)}$ and $K_{opt}$. The obtained analytic solution is plotted in Fig. 4 as solid lines. At the critical control amplitude $K^{(fl)}$ the real part, $\Lambda$, of the Floquet exponent becomes negative giving rise to stabilisation of the formerly unstable orbit. Due to an imaginary part of $\Omega = \pi/\tau$ the stabilisation occurs via an inverse period doubling/flip bifurcation. On further increase of the control amplitude $\Lambda$ decreases until a frequency splitting occurs at $K_{opt}$. Beyond $K_{opt}$ the frequency $\Omega$ deviates from its optimal value $\pi/\tau$, which is accompanied by a re–increase of $\Lambda$. Finally at $K^{(ho)}$ $\Lambda$ may become positive again via a Hopf bifurcation leading to quasiperiodic time behaviour. The described phenomena can also be seen in the frequency spectra of the system variable $U(t)$ for various values of the control amplitude (cf. Fig. 5).

The simple control scheme (2) is restricted to small Lyapunov exponents $\lambda$ or short periods $T$. This limitation can be relaxed by employing multiple delay terms in the control force as in the case of extended time delay autosynchronisation [7], where it is also possible to calculate the stability domain $[K^{(fl)}, K^{(ho)}]$ analytically [8]. Experimental results for three different driving amplitudes $U_A$, corresponding to three different Lyapunov exponents, are displayed in Fig. 6. The fit of the analytical results yields perfect agreement for $K^{(fl)}$ while we observe deviations for $K^{(ho)}$ owing to the crude first–order approximation of our analytical result.

The analytical results yield a general relation between the two critical control amplitudes $K^{(fl)}$, $K^{(ho)}$, the memory parameter $R$ and the frequency deviation $\Phi = \Omega\tau - \pi$ at $K^{(ho)}$, which does not contain any system parameter. Experimental data obtained from the control of an unstable period–4 orbit are presented in Fig. 7.

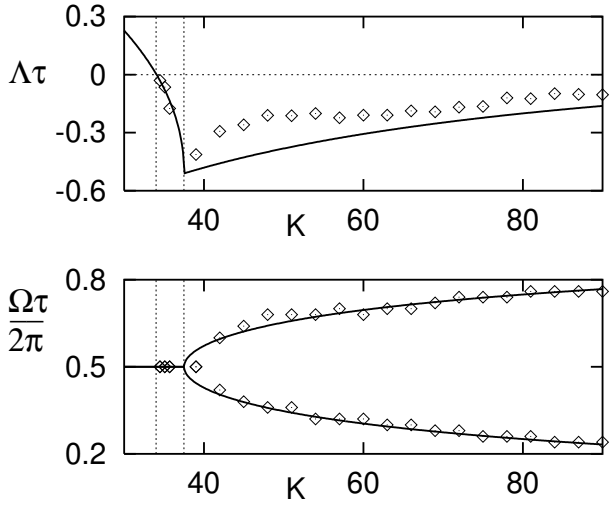


Figure 4: Dependence of Floquet exponent on control amplitude.

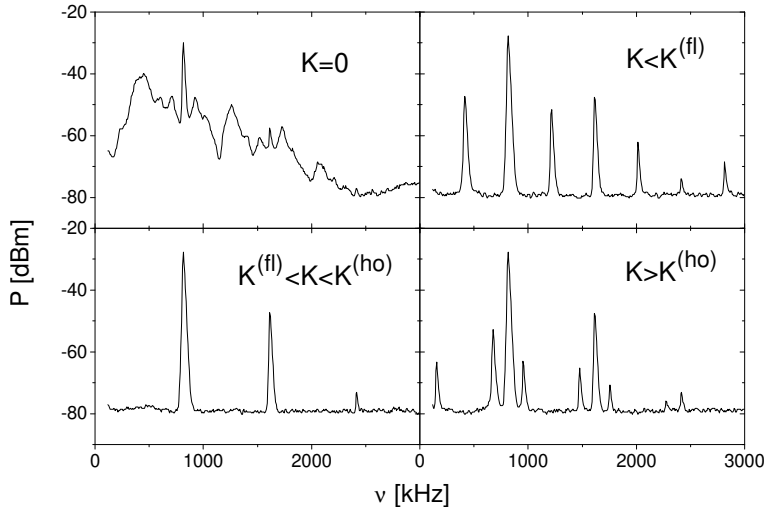


Figure 5: Power spectra of system output for different control amplitudes.

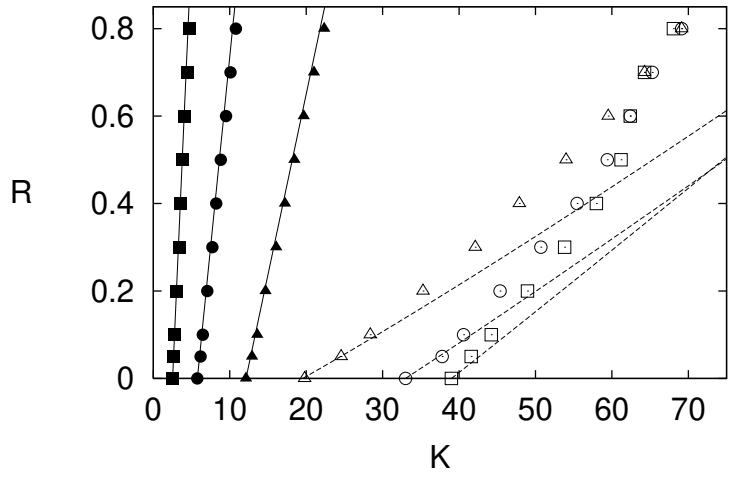


Figure 6: Stability range in the $K$–$R$ parameter plane for three values of the driving amplitude: □ 0.8V, ∘ 1.1V, △ 3.5V. Full/open symbols correspond to the flip/Hopf boundary. Solid/dashed lines indicate the analytical result.

Keeping in mind that the corresponding analytical curves are obtained without any fit parameter the coincidence is remarkable. Hence, the essential qualitative and several quantitative features which determine the stability domain for time–delayed feedback control can already be described by our first–order analysis.

### *3.2 Rössler–type electronic circuit*

Further features of time–delayed feedback control were probed on a Rössler–type nonlinear circuit, consisting of several operational amplifiers with associated feedback components (cf. Fig. 8). The nonlinearity is provided by the diodes. The voltages probed at $x, y, z$ can be considered as the degrees of freedom in our experiment. At $f_x, f_y, f_z$ external signals can be fed into the system for control purpose. Typical frequencies of the circuit are about 600kHz.

Without control the system undergoes a period–doubling cascade to chaos on variation of the resistance $R_V$, ending up in a chaotic attractor. The following measurements have been performed at $R_V = 110\Omega$ were the chaotic attractor contains an unstable period–1 orbit with period $T = 1.656\mu$s and Floquet frequency $\omega = \pi/T$. The delay time $\tau$ was adjusted according to the orbit's period $T$. Here, we only present results obtained for memory parameter $R = 0$. Our feedback scheme consisted of coupling the voltage at $z$ via the control device to $f_z$.

Apart from studying methods of fine adjustment of the delay time $\tau$ in autonomous systems [9] we used this circuit to investigate the influence of control loop latency $\delta$ on the efficiency of control. This additional delay which acts on the control force leads

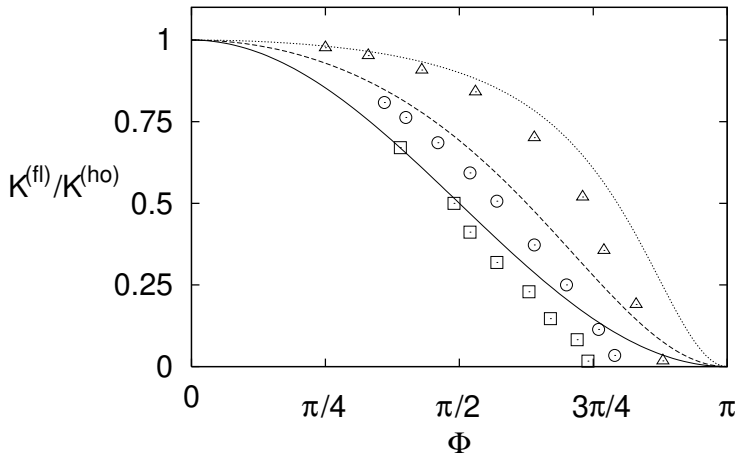


Figure 7: Ratio of critical control amplitudes in dependence on the frequency deviation $\Phi$ at the Hopf instability for several values of $R$. Symbols are results of the electronic circuit experiment, lines display the analytical expression: $R = 0$ ($\square$, solid line), $R = 0.2$ ($\circ$, dashed line), and $R = 0.5$ ($\triangle$, dotted line).

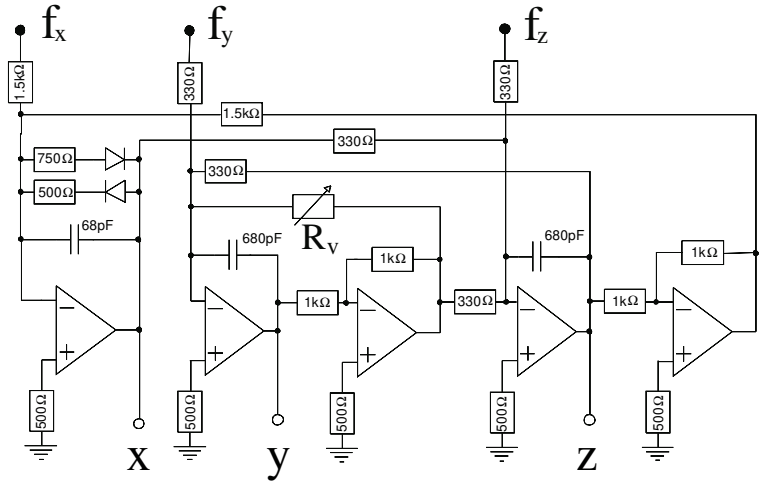


Figure 8: Experimental setup of the nonlinear electronic circuit without the time–delayed feedback device. Experiments have been performed at $R_V = 110\Omega$.

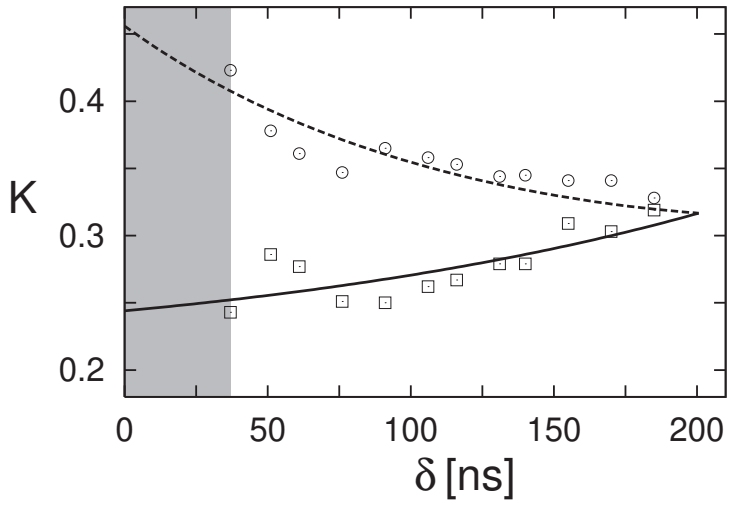


Figure 9: Dependence of control interval on control loop latency, □: $K^{(fl)}(\delta)$, ∘: $K^{(fl)}(\delta)$. The gray–shaded region is not accessible in our experiments due to the intrinsic latency $\delta_0$. The lines are fits of the analytical result to the experimental data.

to a shrinking control interval by shifting the frequency splitting point $K_{opt}$. This phenomenon has been analysed analytically in [10] and it was possible to determine a critical value $\delta_c = \tau(1 - \lambda\tau/2)/(\lambda\tau)$ where stabilisation is no longer achieved. Moreover we note that there always exists a $\delta$–interval within $[n\tau, (n+1)\tau]$ where control will fail.

The latency effect was realized by including an additional delay line between control device and feedback input. The control loop without additional delay line had a latency $\delta_0 = 37$ns. Therefore, by means of this additional device we could systematically investigate latencies $\delta = \delta_0 + \delta_{DL}$, where $\delta_{DL}$ could be set in steps of 1ns. At fixed $\delta$ we swept the control amplitude $K$ to obtain the control interval $[K^{(fl)}, K^{(ho)}]$. The results for different values of $\delta$ are shown in Fig. 9. It is evident that the region of successful control is strongly affected by latency leading to a loss of control for $\delta/\tau \approx 11\%$. The solid and dashed lines are fits to the analytical results of [10] for $K^{(fl)}$ and $K^{(ho)}$, respectively.

### *3.3 Spin–wave instabilities in YIG spheres*

High power ferromagnetic resonance experiments were performed on spheres of yttrium iron garnet (YIG), which is well established as a "prototype nonlinear ferromagnet". The sample was placed in a microwave cavity and excited by a microwave field of 9.39 GHz, applied perpendicularly or parallel to the static magnetic field (cf. Fig. 10). The parametric excitation of spin waves was observed in *subsidiary ab-*

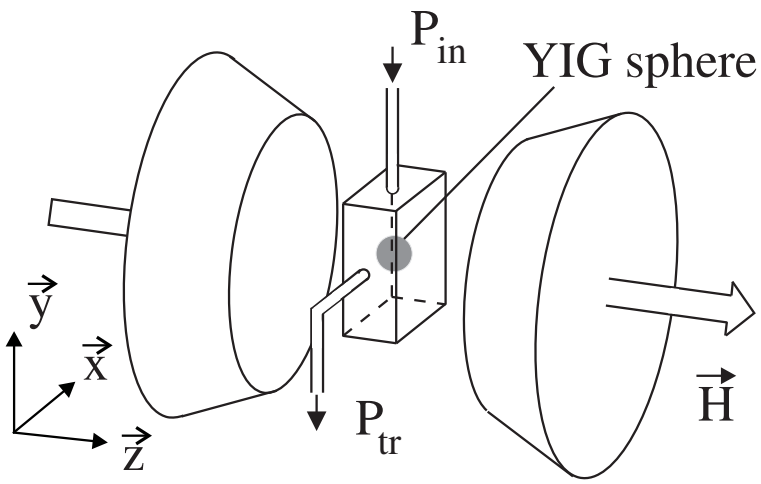


Figure 10: Experimental setup for probing spin–wave instabilities in YIG spheres.

*sorption* and *parallel pumping* (see e.g. [11]). Increasing the pumping power above the instability threshold we observed auto–oscillations and a variety of routes into chaos: period doubling, quasi–periodicity, and different types of intermittency [12]. The auto–oscillation frequencies lie in the MHz range and change dramatically on variation of system parameters making the $\tau$ adjustment a challenge. For the given setup an intrinsic control loop latency of about 70ns was observed.

To illustrate the applicability of the delayed feedback control method to complex spin systems, as a first step we considered a *stable* period–2 orbit (Fig. 11, $K = 0$), which was generated through a period doubling, leaving an unstable period–1 orbit with flipping neighbourhood ($\omega = \pi/T$). This unstable orbit was selected for control. The delay time $\tau = 2.09\mu$s was evaluated from the very sharp and dominating peak in the spectrum. Turning on the feedback and increasing the control amplitude $K$, we observed a changeover to period–1 (Fig. 11, $K = 0.2$), while the period–2 component was suppressed by more than 20dB. The vanishing control signal (below a noise level of about 1% of the diode signal) indicated successful control. On further increase of $K$, the orbit was destabilised again. A widening of the attractor occurred, accompanied by a Hopf bifurcation which resulted in an additional broad peak at about 1.53MHz (Fig. 11, $K = 0.5$). According to the theoretical expectations, there is a $K$–window of successful control which is limited at low $K$–values by a flip bifurcation and at high $K$–values by a Hopf bifurcation.

The following control experiments on marginal chaos did not fully reach this quality of regular signals. We looked for a parameter range where chaos evolves via a period doubling, leading to a flipping neighbourhood ($\omega = \pi/T$), but was followed by two Hopf bifurcations. A proper starting value for the cycle time $\tau = 2.08\mu$s was obtained from the unperturbed spectrum, (Fig. 12, $K = 0$). The unperturbed

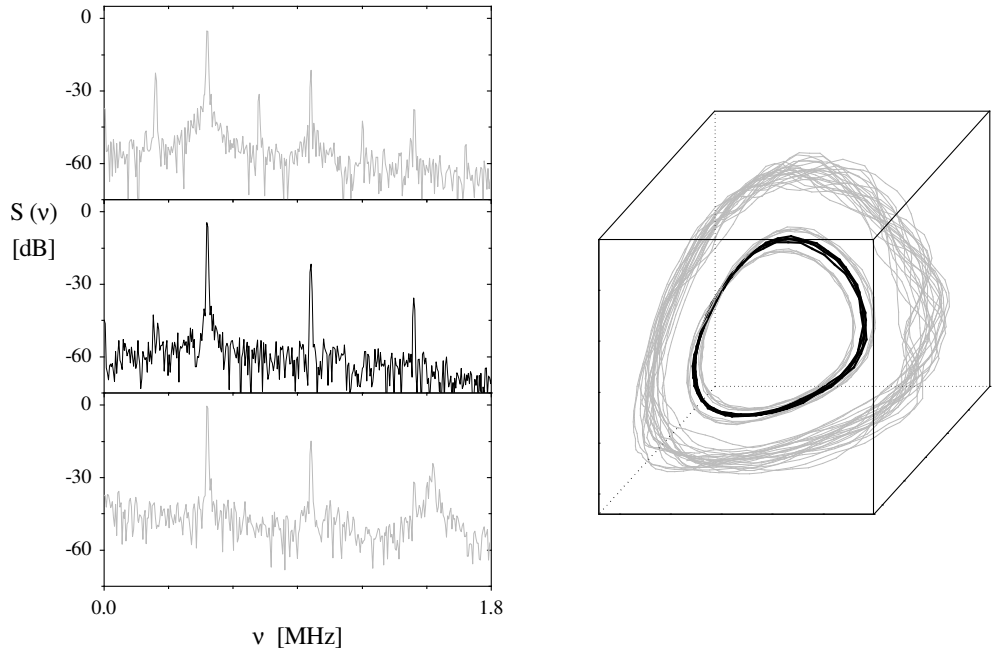


Figure 11: Suppression of a period–2 orbit (parallel pumping, $\nu = 9.39$GHz, $P_{in} = 13.3$dB, $H = 1613$Oe ). L.h.s. top to bottom: stable period–2 orbit ($K = 0$), controlled period–1 orbit ($K = 0.2$), feedback induced torus ($K = 0.5$). R.h.s.: corresponding phase space representations. Note that the stabilised UPO (dark) is located close to the starting period–2 orbit, while for large $K$ an attractor widening occurs.

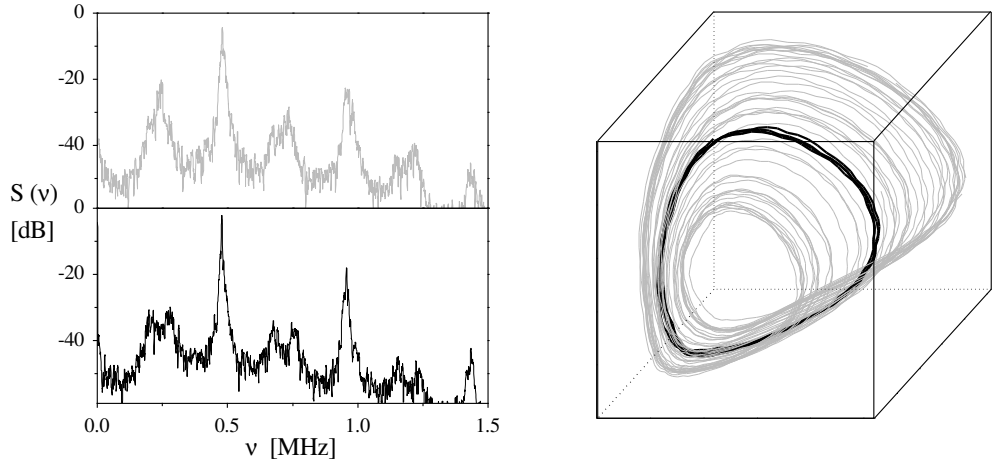


Figure 12: Suppression of chaos (subsidiary absorption, $\nu = 9.39$GHz, $P_{in} = 8.5$dB, $H = 1865$Oe ). L.h.s. top to bottom: chaotic attractor ($K = 0$), stabilised period–1 orbit ($K = 0.37$). R.h.s.: corresponding phase space representations. Note that the stabilised periodic orbit (dark) is embedded in the chaotic attractor.

spectrum again shows a noisy but pronounced period–2 component. Applying a moderate feedback amplitude ($K = 0.37$), the irregular behaviour is largely suppressed (Fig. 12). The period–1 peak becomes rather narrow, the period–2 fluctuations are decreased by about 15dB, while the frequency components which resulted from the Hopf bifurcations are less affected.

These experiments show that chaotic spin systems, in spite of their complexity and fast time scale, can be controlled by time–delayed feedback technique. General properties and limitations of this technique, as predicted from a system–independent theory, show up very distinctly in our experimental findings.

## 4 Conclusion

Time–delayed feedback control is a useful and easily implemented tool to control periodic orbits in complex dynamical systems. Both thorough experimental investigations and theoretical analyses are necessary for an understanding of the control features and a finally successful application of the method. Several general features, which are valid beyond our special experimental setups have been worked out:

- Torsion is a necessary condition for delayed feedback schemes to work at all. In particular, in low dimensional dissipative systems only flip orbits are accessible to control, and the control interval is bounded by flip and Hopf bifurcations [5]. As a consequence one enters the control interval via an inverse period doubling sequence at low control amplitudes. At large control amplitudes control fails again and incommensurate frequencies appear in the spectrum of the signal.

- Control domains become small and finally may even vanish, if orbits with long periods or large Lyapunov exponents are considered [8]. Such a limitation may be overcome by employing multi–delay schemes like the extended autosynchronisation introduced in [7]. Even these improved schemes are simple to apply since just a single additional delay line is required.

- Control loop latency is an important restriction for every control scheme. Such features have been known by engineers for decades [13]. Since delayed feedback schemes are in particular designed for ultrafast experiments such limitations may become crucial and a critical latency seems to exist beyond which no control is possible [10]. Unfortunately one cannot expect that multi–delay schemes improve such restrictions considerably.

- The proper adaptation of delay time is crucial in order that the control signal vanishes. Such an adaptation is usually no problem in nonautonomous systems, but may cause considerable problems in the autonomous case if the periods of the orbits are not known a priori. Some semi–empirical schemes have been developed to cope with such problems [14]. However a closer theoretical inspection

along the lines of section 2 reveals that properties of the control signal can be used in a systematic way to derive proper delay times from properties of the control signal [9].

- Finally, even the limitation caused by the torsion of the orbits can in principle be avoided by applying time dependent control amplitudes [15]. Such schemes have been investigated in the context of maps [16] but real applications are still missing since not all features seem to be well understood so far.

Although our understanding of control features has considerably increased during the last years there remains a lot of work to be done. In particular, control of high–dimensional systems is just at the beginning of being understood. Even in that context time–delayed feedback schemes might prove to be useful, as indicated by variants including spatial delays, [17]. but at the moment no definite conclusions can be drawn. Finally one should keep in mind that there is a simple criterion which indicates the effectiveness of any control method, namely its success in real experimental applications.

## References


[1] E. Ott, C. Grebogi, and Y. A. Yorke, Phys. Rev. Lett. **64** (1990) 1196

[2] H. Kantz and T. Schreiber, *Nonlinear time series analysis*, (Camb. Univ. Press, Cambridge, 1997)

[3] K. Pyragas, Phys. Lett. A **170** (1992) 421

[4] S. Bielawski, D. Derozier, and P. Glorieux, Phys. Rev. E **49** (1994) R971
T. Pierre, G. Bonhomme, and A. Atipo, Phys. Rev. Lett. **76** (1996) 2290
T. Hikihara, M. Touno, and T. Kawagoshi, Int. J. Bif. Chaos **7** (1997) 2837

[5] W. Just, T. Bernard, M. Ostheimer, E. Reibold, and H. Benner, Phys. Rev. Lett. **78** (1997) 203

[6] H. Nakajima, Phys. Lett. A 232 (1997) 207

[7] J. E. S. Socolar, D. W. Sukov, and D. J. Gauthier, Phys. Rev. E **50** (1994) 3245

[8] W. Just, E. Reibold, H. Benner, K. Kacperski, P. Fronczak, and J. Hołyst, Phys. Lett. A **254** (1999) 158

[9] W. Just, D. Reckwerth, J. Möckel, E. Reibold, and H. Benner, Phys. Rev. Lett. **81** (1998) 562

[10] W. Just, D. Reckwerth, E. Reibold, and H. Benner, Phys. Rev. E **59** (1999) 2826

[11] *Nonlinear Phenomena and Chaos in Magnetic Materials*, edited by P.E. Wigen (World Scientific, Singapore, 1994)

[12] J. Becker, F. Rödelsperger, Th. Weyrauch, H. Benner, W. Just, and A. Čenys, Phys. Rev. E **59** (1999) 1622

[13] L. Collatz, Z. angew. Math. Mech. **25/27** (1947) 60

[14] A. Kittel, J. Parisi, and K. Pyragas, Phys. Lett. A **198** (1995) 433; H. Nakajima, H. Ito, and Y. Ueda, IEICE Trans. Fund. **E80** (1997) 1554

[15] S. Bielawski, D. Derozier, and P. Glorieux, Phys. Rev. A **47** (1993) 2492

[16] H. G. Schuster and M. B. Stemmler, Phys. Rev. E **56** (1997) 6410

[17] A. V. Mamaev and M. Saffman, Phys. Rev. Lett. **80** (1998) 3499